Current density waves in open mesoscopic rings driven by time-periodic magnetic fluxes

2010 J. Phys.: Condens. Matter 22 185301

(http://iopscience.iop.org/0953-8984/22/18/185301)

J. Phys.: Condens. Matter **22** (2010) 185301 (6pp) doi:10.1088/0953-8984/22/18/185301

Current density waves in open mesoscopic rings driven by time-periodic magnetic fluxes

Cong-Hua Yan[1,2] **and Lian-Fu Wei**[1]

[1] Quantum Optoelectronics Laboratory, Southwest Jiaotong University, Chengdu 610031, People's Republic of China
[2] College of Physics and Electronic Engineering, Sichuan Normal University, Chengdu 610068, People's Republic of China

E-mail: weilianfu@gmail.com

Received 1 December 2009, in final form 21 March 2010
Published 15 April 2010
Online at stacks.iop.org/JPhysCM/22/185301

Abstract
Quantum coherent transport through open mesoscopic Aharonov–Bohm rings (driven by static fluxes) have been studied extensively. Here, by using quantum waveguide theory and the Floquet theorem we investigate the quantum transport of electrons along an open mesoscopic ring threaded by a *time-periodic* magnetic flux. We predicate that current density waves could be excited along such an open ring. As a consequence, a net current could be generated along the lead with only one reservoir, if the lead additionally connects to such a normal-metal loop driven by the *time-dependent* flux. These phenomena could be explained by photon-assisted processes, due to the interaction between the transported electrons and the applied oscillating external fields. We also discuss how the time-average currents (along the ring and the lead) depend on the amplitude and frequency of the applied oscillating fluxes.

1. Introduction

Recently, the subject of time-dependent transport of electrons through various nanostructures has attracted increasing attention. This topic is concerned with certain controllable transport phenomena, which have potential applications to various nano-electronic devices [1].

In the time-dependent driving process, the applied external oscillating perturbations affect the phase factors of the wavefunctions in different regions, inducing the well-known photon-assisted tunneling (PAT) [2]. Basically, PAT is a process in which an oscillating potential can lead to energy exchanges between the electrons and energy quanta (photons) of the applied oscillating field, and thus yield the desirable electron tunnelings. For example, an harmonically driven potential could result in energy exchange between the electrons and the applied external field in units of 'photon' quanta $\hbar\omega$, with ω being the modulating frequency of the applied harmonic field. Consequently, electrons inputting at energy E can be transferred to sidebands with energies $E \pm n\hbar\omega$ ($n = 0, \pm1, \pm2, \ldots$).

Experimentally, PATs had been observed in terms of resonant tunnelings through certain electronic structures, such as quantum wells [3], quantum dots [4], quantum diodes [5], and semiconductor superlattices [6]. In fact, PATs had been utilized to design various high-speed switching devices and high-frequency radiation sources and detectors [5]. More recently, it is theoretically predicted that PATs could also reveal in current nano-scale structures, e.g. *spinor* quantum wells [7, 8], mesoscopic hybrid systems [9], carbon nanotubes [10–12], graphenes [13, 14], etc.

Typically, the studies of electronic transports in mesoscopic rings threaded by time-dependent fluxes are relatively new [15]. It is expected that electronic transports along these topologically nontrivial structures could reveal certain new phenomena. For example, Shin and Hong [16, 17] discussed the transport of electrons along a nanostructure of connected double-rings with two leads; each ring is threaded by both static and dynamically changed fluxes. They showed that electron pumping could be implemented by using the PAT along such a double-ring structure, and also the generated PAT process could be utilized to filter the momentum of transported electrons.

In the present work, we consider the PAT process through an open mesoscopic ring driven by a time-periodic flux and coupled to a reservoir via an ideal one-dimensional metal lead.

This structure driven by only the static flux has already been investigated [18, 19]. In this case the reflection probability of the electrons (injected from the reservoir and reflected by the ring) in the lead is always equal to one, and thus the current in the lead is zero. This indicates that the applied static flux does not influence the electron transporting along the lead. However, when the ring is threaded by time-dependent magnetic flux, the current might appear between the reservoir and the open ring. For example, Arrachea *et al* [20] showed theoretically that a tunneling current appears when the ring is threaded by a linearly varying flux. In particular, under the so-called *few-sideband approximation* (i.e. only a few sidebands, for example the lowest three sidebands, were considered), Büttiker [21] had originally treated the case wherein the ring is threaded by a time-periodically changed flux.

Here, without making use of any approximation we exactly treat such a problem in the framework of Floquet scattering theorem [22–25] and time-dependent quantum waveguide theory [26–30]. Various inelastic scatterings between photon sidebands (i.e. scattering channels) will be *completely* considered. Our numerical results show very clearly that the current flowing along the lead indicates the appearance of PAT phenomena. How the amplitude and frequency of the applied oscillating fluxes influence these PAT phenomena is also discussed.

2. Model

The nanostructure we consider here is shown in figure 1, where a single open mesoscopic ring is driven by both the static and dynamic fluxes and coupled to a reservoir via a lead. To simplify it, we neglect electron–electron and electron–phonon interactions. Therefore, the motion of electrons along the lead is free, while that in the ring region is described by the Hamiltonian

$$H(x,t) = -\frac{\hbar^2}{2m_e}\left[\frac{\partial}{\partial x} - i\frac{2\pi}{L}\Phi(t)\right]^2 = H_0(x) + V(x,t), \tag{1}$$

where m_e is the mass of the electron, L is the circumference of the ring, and $\Phi(t) = f_s + f_d\cos(\omega t)$ is the oscillating magnetic flux expressed in units of the flux quantum h/e, with f_s being the static component and f_d being the amplitude of the dynamic component. The oscillating flux $f_d\cos(\omega t)$ affects the transport properties of the ring in the same way as the oscillating potential in the potential structures, and simulates the process of phase-coherent inelastic scattering [31].

The solutions to the time-dependent Schrödinger equation with the above Hamiltonian (1) can be obtained by using the well-known Floquet theorem [25], a temporal version of the Bloch theorem. This theorem says that the wavefunction $\Psi(x,t)$ of a periodically driven quantum system could be formally represented as

$$\Psi(x,t) = e^{-iE_{fl}t/\hbar}\phi(x,t), \qquad \phi(x,t) = \phi(x,t+2\pi/\omega), \tag{2}$$

with E_{fl} being the so-called Floquet energy. Substituting $\Psi(x,t)$ into the time-dependent Schrödinger equation gives

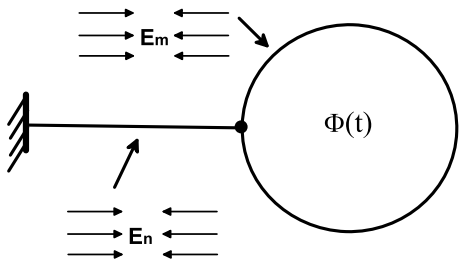

Figure 1. Schematic diagram of a mesoscopic one-dimensional normal conductor ring driven by a time-periodically changed flux and coupled with a reservoir via an ideal one-dimensional lead: $\Phi(t) = f_s + f_d\cos(\omega t)$. Energies of the incoming and outgoing waves (sidebands) are represented in terms of the Floquet zones with the unit of $\hbar\omega$. E_n denotes the sub-sidebands in the lead, while E_m represents the sub-sidebands in the ring.

rise to an eigenvalue equation

$$E_{fl}\phi(x,t) = \left[H(x,t) - i\hbar\frac{\partial}{\partial t}\right]\phi(x,t). \tag{3}$$

Furthermore, it is assumed that the function $\phi(x,t)$ can be written as a time–space separable form, $\phi(x,t) = \sum_k a_k f_k(t) g_k(x)$, with $g_k(x)$ being the wavevector-dependent functions required to be determined later, and

$$f_k(t) = e^{-\frac{i}{\hbar}[\varepsilon t - \alpha_k \sin(\omega t) + \frac{r}{2\omega}\sin(2\omega t)]}. \tag{4}$$

Here, $\varepsilon = \hbar^2k^2/(2m_e) + r - E_{fl}$, $r = \pi^2\hbar^2 f_d^2/(m_e L^2)$, and $\alpha_k = 2k\pi\hbar^2 f_d/(m_e L\omega)$. The periodic characteristic of $\phi(x,t)$, i.e. $\phi(x,t) = \phi(x,t+2\pi/\omega)$, yields

$$f_k(t+2\pi/\omega) = f_k(t)e^{-\frac{i\varepsilon 2\pi}{\hbar\omega}}. \tag{5}$$

This constrains the values of the effective energies and relevant wavevectors as: $\varepsilon = m\hbar\omega$ and $\hbar k_m = \sqrt{2m_e(E_{fl} + m\hbar\omega - r)}$, respectively. Here, m is an integer marking the Floquet sidebands. The negative integer m corresponds to the so-called evanescent modes [32], which do not contribute to the current on the lead. However, these modes should be taken into account in treating the present system containing various inelastic scatterings.

Expressing the time-dependent parts in terms of Bessel functions, $\exp[z(\mu - 1/\mu)/2] = \sum_n J_n(z)\mu^n$, with $J_n(z)$ being the ordinary Bessel function of order n [33], the wavefunction in the ring region takes the form:

$$\Psi^R(x,t) = \sum_{m,n,l}[a_m e^{iK_m^+ x} + b_m(-1)^{m-n}e^{-iK_m^-(x-L)}] \times J_{m-n+2l}\left(\frac{\alpha_k}{\hbar}\right)J_l\left(\frac{r}{2\hbar\omega}\right)e^{iF(t)}. \tag{6}$$

In this equation, $F(t) = -(E_{fl} + n\hbar\omega)t/\hbar$ and $K_m^\pm = k_m \pm 2\pi f_s/L$. Since electrons incident to the oscillating region could be scattered into different Floquet sidebands, the wavefunctions outside the ring must be composed of a series of Floquet sidebands in order to match the boundary conditions at the junction. We assume that the particle waves of the lead are the superpositions of an infinite number of sidebands with

energies spacing with $\hbar\omega$. The potential in the lead is zero, so the wavefunction on it can be written as

$$\Psi^{\mathrm{L}}(x,t) = \mathrm{e}^{\mathrm{i}q_0 x}\mathrm{e}^{-\mathrm{i}E_{i0}t/\hbar} + \sum_n r_{n0}\mathrm{e}^{-\mathrm{i}q_n x}\mathrm{e}^{-\mathrm{i}E_n t/\hbar}. \quad (7)$$

Above, r_{n0} is the reflection probability amplitude of incoming waves from the left lead to the ring. The above equation also involves modes with energies below E_{i0} (in the sum, n can be negative). The evanescent modes (with $E_n < 0$) neither propagate nor contribute to the transported currents, as the wavevectors $q_n = \sqrt{2m_{\mathrm{e}}E_n/\hbar^2}$ of these modes are imaginary.

The unknown coefficients in the above wavefunctions can be determined by using the boundary conditions of the wavefunctions, i.e. they and their first derivatives must be continuous at the junction. Thus, at the junction we have $\Psi^{\mathrm{L}}(0,t) = \Psi^{R}(0,t) = \Psi^{R}(L,t)$, $\partial\Psi^{\mathrm{L}}(x,t)/\partial x|_{x=0} = \partial\Psi^{R}(x,t)/\partial x|_{x=0} - \partial\Psi^{R}(x,t)/\partial x|_{x=L}$. These boundary conditions yield

$$\begin{aligned}\delta_{n0} + r_{n0} &= \sum_{m,l}[a_m + b_m(-1)^{m-n}\mathrm{e}^{\mathrm{i}K_m^- L}]J \\ &= \sum_{m,l}[a_m\mathrm{e}^{\mathrm{i}K_m^+ L} + b_m(-1)^{m-n}]J, \end{aligned} \quad (8)$$

and

$$\begin{aligned}q_n\delta_{n0} - q_n r_{n0} = \sum_{m,l}[&a_m K_m^+ - b_m K_m^-(-1)^{m-n}\mathrm{e}^{\mathrm{i}K_m^- L} \\ &- a_m K_m^+\mathrm{e}^{\mathrm{i}K_m^+ L} + b_m K_m^-(-1)^{m-n}]J, \end{aligned} \quad (9)$$

respectively. Above, the parameter J is defined by

$$J = J_{m-n+2l}\left(\frac{\alpha_k}{\hbar}\right)J_l\left(\frac{r}{2\hbar\omega}\right). \quad (10)$$

We can eliminate the parameters r_{n0} and obtain

$$\begin{aligned}2q_n\delta_{n0} = \sum_{m,l}[&a_m(K_m^+ + q_n) + b_m(q_n - K_m^-)(-1)^{m-n}\mathrm{e}^{\mathrm{i}K_m^- L} \\ &- a_m K_m^+\mathrm{e}^{\mathrm{i}K_m^+ L} + b_m K_m^-(-1)^{m-n}]J, \end{aligned} \quad (11)$$

and

$$\begin{aligned}2q_n\delta_{n0} = \sum_{m,l}[&a_m K_m^+ - b_m K_m^-(-1)^{m-n}\mathrm{e}^{\mathrm{i}K_m^- L} \\ &+ a_m(q_n - K_m^+)\mathrm{e}^{\mathrm{i}K_m^+ L} + b_m(q_n + K_m^-)(-1)^{m-n}]J, \end{aligned} \quad (12)$$

respectively.

In practice, these equations need to be expressed in the matrix form:

$$\begin{aligned} M_0M_1 = M_2A + M_3B \qquad M_0M_1 = M_4A + M_5B \\ M_1 + M_r = M_aA + M_bB, \end{aligned} \quad (13)$$

and the square matrices are defined by the matrix elements: $M_{0nm} = 2q_n\delta_{nm}$, $M_{anm} = J$, $M_{bnm} = (-1)^{m-n}\mathrm{e}^{\mathrm{i}K_m^- L}J$, $M_{2nm} = \sum_l(q_n + K_m^+ - K_m^+\mathrm{e}^{\mathrm{i}K_m^+ L})J$, $M_{3nm} = \sum_l[(q_n - K_m^-)\mathrm{e}^{\mathrm{i}K_m^- L} + K_m^-](-1)^{m-n}J$, $M_{4nm} = \sum_l[K_m^+ + (q_n - K_m^+)\mathrm{e}^{\mathrm{i}K_m^+ L}]J$, and $M_{5nm} = \sum_l(-K_m^-\mathrm{e}^{\mathrm{i}K_m^- L} + q_n + K_m^-)(-1)^{m-n}J$.

The column matrices are denoted by the matrix elements: $A_n = a_n$, $B_n = b_n$, $M_{1n} = \delta_{n0}$, and $M_{rn} = r_{no}$. From the matrix equation, one can obtain the matrices of the reflection amplitude and the coefficients of the wavefunction in the ring region.

$$\begin{aligned} M_r = [&M_aM_2^{-1}M_0 - 1 - (M_aM_2^{-1}M_3 - M_b) \\ &\times (M_2^{-1}M_3 - M_4^{-1}M_5)^{-1}(M_2^{-1} - M_4^{-1})M_0]M_1 \end{aligned} \quad (14)$$

$$\begin{aligned} A = [&M_2^{-1} - M_2^{-1}M_3(M_2^{-1}M_3 - M_4^{-1}M_5)^{-1} \\ &\times (M_2^{-1} - M_4^{-1})]M_0M_1 \end{aligned} \quad (15)$$

$$B = [M_2^{-1}M_3 - M_4^{-1}M_5]^{-1}(M_2^{-1} - M_4^{-1})M_0M_1. \quad (16)$$

Based on the matrix M_r, we can get the total electron-reflection probability R of one incident electron as

$$R = \sum_{n=0}^{\infty}|r_{n0}|^2. \quad (17)$$

3. Current density waves in the open mesoscopic rings

With the above wavefunctions, the time- and space-dependent current densities $J_{\mathrm{ring}}(x,t)$ and $J_{\mathrm{lead}}(x,t)$ in the open ring and lead could be easily calculated as

$$\begin{aligned} J_{\mathrm{ring}}(x,t) = &\frac{e\hbar}{m_{\mathrm{e}}}\sum_{m,n,l}k_m(|a_m|^2 - |b_m|^2)J^2 \\ &- \frac{e\hbar}{m_{\mathrm{e}}}\sum_{m,n,l}\frac{2\pi f_{\mathrm{d}}\cos(\omega t)}{L}[|a_m|^2 + |b_m|^2 \\ &+ a_m b_m^*(-1)^{m-n}\mathrm{e}^{\mathrm{i}(k_m + \frac{2\pi f_{\mathrm{s}}}{L})x}\mathrm{e}^{\mathrm{i}(k_m - \frac{2\pi f_{\mathrm{s}}}{L})(x-L)} \\ &+ b_m a_m^*(-1)^{m-n}\mathrm{e}^{-\mathrm{i}(k_m + \frac{2\pi f_{\mathrm{s}}}{L})x} \\ &\times \mathrm{e}^{-\mathrm{i}(k_m - \frac{2\pi f_{\mathrm{s}}}{L})(x-L)}]J^2 \end{aligned} \quad (18)$$

$$\begin{aligned} J_{\mathrm{lead}}(x,t) = \frac{e\hbar q_0}{m_{\mathrm{e}}}\Bigg[&1 - \sum_n\frac{q_n}{q_0}|r_{n0}|^2 + \sum_n\left(1 - \frac{q_n}{q_0}\right) \\ &\times \langle\cos[(E_n - E_{i0})t/\hbar]\{\mathrm{Re}\,r_{n0}\cos[(q_n + q_0)x] \\ &+ \mathrm{Im}\,r_{n0}\sin[(q_n + q_0)x]\} + \sin[(E_n - E_{i0})t/\hbar] \\ &\times \{-\mathrm{Re}\,r_{n0}\sin[(q_n + q_0)x] + \mathrm{Im}\,r_{n0}\cos[(q_n + q_0)x]\}\rangle\Bigg] \end{aligned} \quad (19)$$

where the $\mathrm{Re}\,r_{n0}$ ($\mathrm{Im}\,r_{n0}$) is the real part (the image part) of the reflection matrix element. Obviously, these are wave behaviors with 'frequency' ω.

Without loss of generality for numerical calculations, we consider a single electronic wave incident from one direction (for example, from the left to the ring) with a fixed energy $E = E_{i0} = E_{\mathrm{fl}}$ [25]. For convenience, the parameters in equations (6) and (7) are re-expressed as: $Lq_n = \pi\sqrt{2E_n/E_0}$, $Lk_m = \pi\sqrt{2(E_{\mathrm{fl}} + m\hbar\omega - r)/E_0}$, and $r/(2\hbar\omega) = f_{\mathrm{d}}^2E_0/(2\hbar\omega)$, $\alpha_k/\hbar = 2f_{\mathrm{d}}\sqrt{k^2\hbar^2E_0/(m_{\mathrm{e}}\hbar^2\omega^2)} \approx 2f_{\mathrm{d}}\sqrt{E_{\mathrm{F}}E_0}/(\hbar\omega)$, respectively, and we also choose $E_0 = \hbar^2\pi^2/(m_{\mathrm{e}}L^2)$ as a typical unit of energy. Due to the fact that integers m, n are infinite, we need to solve, in principle, infinite equations relating to the infinite coefficients a_m and b_m. An appropriate upper bound may be given by the asymptotic behavior of the Bessel function of large order [33], such as

$$J_v(z) \approx \frac{1}{\sqrt{2\pi v}}\left(\frac{\mathrm{e}z}{2v}\right)^v, \quad (20)$$

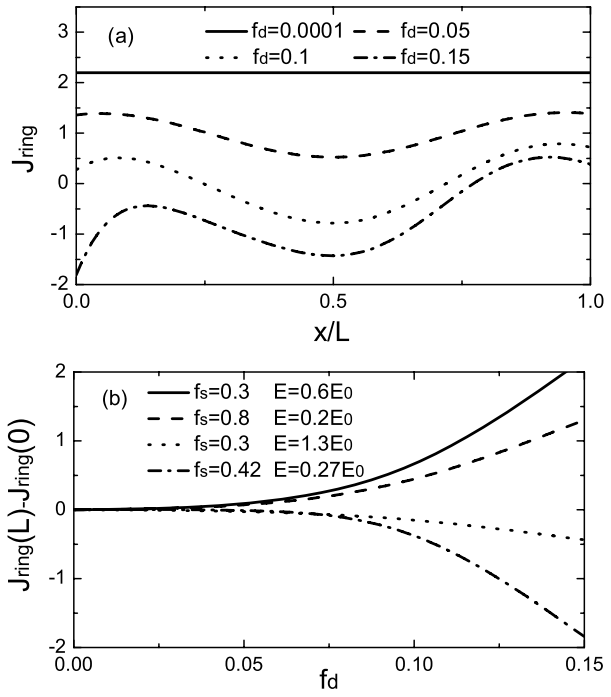

Figure 2. Current density wave along the open mesoscopic ring: (a) space-dependent current density $J_{\rm ring}$ versus x for different dynamic amplitudes of the flux: $f_{\rm d} = 0.0001, 0.05, 0.1, 0.15$ for $f_{\rm s} = 0.3$, $E = 0.6E_0$. The solid line in this figure shows that the current density wave cannot be excited, if the applied oscillating flux is sufficiently weak. (b) The differences between $J_{\rm ring}(L)$ and $J_{\rm ring}(0)$ versus the amplitude $f_{\rm d}$ of the applied oscillating flux. The other parameters are taken as: $t = 2\pi/\omega$, $\hbar\omega = 2E_0$ and $E_{\rm F} = 5\hbar\omega$.

with e being the base of natural logarithm. If $z < 2v_{\rm c}/{\rm e}$, where $v_{\rm c}$ is the cutoff order, the terms with orders higher than $v_{\rm c}$ could be neglected. The parameters $f_{\rm d}$ and $E_{\rm F}$ used in this work are limited within the range $\alpha_k/\hbar < 2$, i.e. $v_{\rm c} > [\sim{\rm e}] = 2$. Since the above Bessel function is fast convergent, it is sufficient to include terms up to $v = 13$ for the numerical calculations [16, 17, 31]. The same upper bound is chosen for the sideband index of the lead.

Typically, figure 2 shows how the current densities are distributed along the ring driven by the time-periodic fluxes. Obviously, for sufficiently weak oscillating flux, e.g. $f_{\rm d} = 0.0001$, the current densities at the different locations are almost the same. This means that the excitation of the current density wave is negligible. For the case with $f_{\rm d} = 0.05$ a current density wave (dash line in figure 2(a)) with a seeming 'wavelength' L is clearly excited along the ring. However, with increasing amplitude of the driven oscillating flux, the space periodicity is broken. Figure 2(b) shows the differences between the two sides of the junction $J_{\rm ring}(L)$ and $J_{\rm ring}(0)$ for the different dynamic drivings. It is seen that, if the driving is almost static: $f_{\rm d} \approx 0$, then $|J_{\rm ring}(L) - J_{\rm ring}(0)| \approx 0$. However, for $f_{\rm d} \gg 0$ we have $|J_{\rm ring}(L) - J_{\rm ring}(0)| \gg 0$, which implies that a net current is induced along the lead, i.e. $|J_{\rm lead}| > 0$. Physically, $J_{\rm ring}(L) \neq J_{\rm ring}(0)$ is relative to the transitions between the sidebands of Floquet energies of the electron in the lead and ring. Those transitions should be enhanced with increasing amplitude of the oscillating drivings.

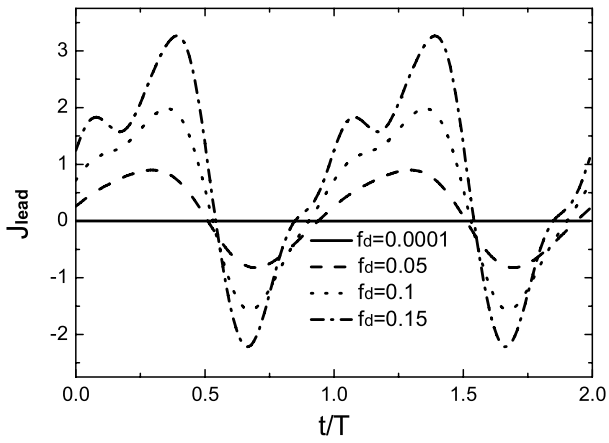

Figure 3. Time-oscillating current densities in the lead for different dynamic driving amplitudes. The parameters involved are: $f_{\rm s} = 0.3$, $E = 2.2E_0$, $\hbar\omega = 2E_0$, $x = 0$, and $E_{\rm F} = 5\hbar\omega$.

Furthermore, figure 3 shows the exact time periodicity of the current densities in the lead for the typical amplitudes $f_{\rm d}$ of the oscillating drivings. It is obviously seen that these current densities have the same period $T = 2\pi/\omega$ as the applied dynamic flux: $f_{\rm d}\cos(\omega t)$. Also, it shows specifically that the amplitude of the induced oscillating current density in the lead increases with the increasing of $f_{\rm d}$. This is assisted by the numerical results shown in figure 2(b).

4. Time average currents in the lead and the ring with a single electron reservoir

We now consider the time average currents [34] over the time-period $T = 2\pi/\omega$ along the lead and ring. First, with the time- and space-dependent current density $J_{\rm lead}(x,t)$ we have

$$\begin{aligned} I_{\rm lead} = \frac{1}{T}\int_0^T J_{\rm lead}(x,t)\,{\rm d}t &= \frac{{\rm e}\hbar q_0}{m_{\rm e}}\left(1 - \sum_n \frac{q_n}{q_0}|r_{n0}|^2\right) \\ &+ \frac{1}{T}\frac{{\rm e}\hbar q_0}{m_{\rm e}}\sum_n\left(1-\frac{q_n}{q_0}\right)\frac{\hbar}{E_n - E_{i0}} \\ &\times \{{\rm Re}\, r_{n0}\cos[(q_n+q_0)x] + {\rm Im}\ r_{n0}\sin[(q_n+q_0)x]\} \\ &\times \sin[(E_n - E_{i0})t/\hbar]|_0^T \\ &+ \frac{1}{T}\frac{e\hbar q_0}{m_{\rm e}}\sum_n\left(1-\frac{q_n}{q_0}\right)\frac{\hbar}{E_n - E_{i0}} \\ &\times \{-{\rm Re}\, r_{n0}\sin[(q_n+q_0)x] + {\rm Im}\ r_{n0}\cos[(q_n+q_0)x]\} \\ &\times (-1)\cos[(E_n - E_{i0})t/\hbar]|_0^T. \end{aligned} \tag{21}$$

According to the Floquet theory used above, $E_n - E_{i0} = n\hbar\omega$, $n = 0, 1, 2, \ldots$, we have $T(E_n - E_{i0})/\hbar = 2\pi/\omega(E_n - E_{i0})/\hbar = 2n\pi$, and thus the above integration finally reduces to the following dc form

$$I_{\rm lead} = \frac{{\rm e}\hbar q_0}{m_{\rm e}}\left(1 - \sum_n \frac{q_n}{q_0}|r_{n0}|^2\right), \tag{22}$$

which is independent of the time and space variables.

Similarly, the average current in the ring region can be denoted as

$$I_{\text{ring}} = \frac{1}{T}\int_0^T J_{\text{ring}}(x,t)\,\mathrm{d}t = \frac{e\hbar}{m_{\text{e}}}\sum_{m,n,l} k_m(|a_m|^2 - |b_m|^2)J^2. \quad (23)$$

It is emphasized that, when the dynamic part of the flux is sufficiently small (and thus the static part of the flux is dominant), the sideband transition between the lead and the driven ring is negligible. In this case, only one sideband is considered and the ordinary Bessel function J closes to unit. As a consequence, the average currents along the ring and lead reduce to

$$I_{\text{ring}} = \frac{e\hbar}{m_{\text{e}}}k_0(|a_0|^2 - |b_0|^2), \quad (24)$$

and

$$I_{\text{lead}} = 0, \quad (25)$$

respectively. These are assisted by the case where only the static flux is applied [19].

Physically, the existence of the sideband transitions is due to the oscillating flux drivings, and the electron could be reflected back to the lead via multiple sidebands. Therefore, the average currents along the lead and ring relate to the reflection coefficient R in equation (17). In figures 4(a)–(c), we plot the reflection coefficient R, the average current in the lead I_{lead} and the average current along the ring as functions of the static magnetic flux f_{s}. It is clearly seen that when the amplitude of the dynamic flux f_{d} is sufficiently small, $R \equiv 1$ and $I_{\text{lead}} \equiv 0$. This implies that, under the weak dynamic flux, the electron injected from the reservoir can not be transported into the ring but will be reflected completely back to the lead [19, 20], which results in the disappearance of the net current along the lead. However, for significantly dynamic drivings, the reflection coefficient R is no longer kept at unity, and thus the average current along the lead might be nonzero. This is because, by interacting with the applied oscillating external field, electrons in the incident channel could emit photons and then drop to the lower sidebands. Similarly, electrons could also absorb photons and then jump to the higher sidebands of the incident channel. The periodic property of current in the lead on the static strength f_{s} comes from the periodic structure of the effective wavevectors: $K_m^{\pm} = k_m \pm 2\pi f_{\text{s}}/L$, with k_m being the wavevector of the mth sideband. We also see from figure 4(c) that, for sufficiently weak dynamic flux, e.g. $f_{\text{d}} = 0.0001$, the average current along the ring shows typical Aharonov–Bohm oscillation. With the increasing of f_{d}, the Aharonov–Bohm peaks are suppressed, as the electron of the ring is scattered out to various sidebands of the lead by the PAT process. Therefore, the time-periodic flux suppresses the Aharonov–Bohm effect related to the usual static flux.

In figure 5, for the typical parameters $E = 2.2E_0$, $f_{\text{d}} = 0.1$ and $E_{\text{F}} = 5\hbar\omega$, we discuss how the frequency of the applied oscillating flux influences the average currents in the lead and along the ring. It is clear that the amplitude of I_{lead} (versus the static flux f_{s}) decreases with the increase of the driven frequency. On the contrary, figure 5(b) shows that the

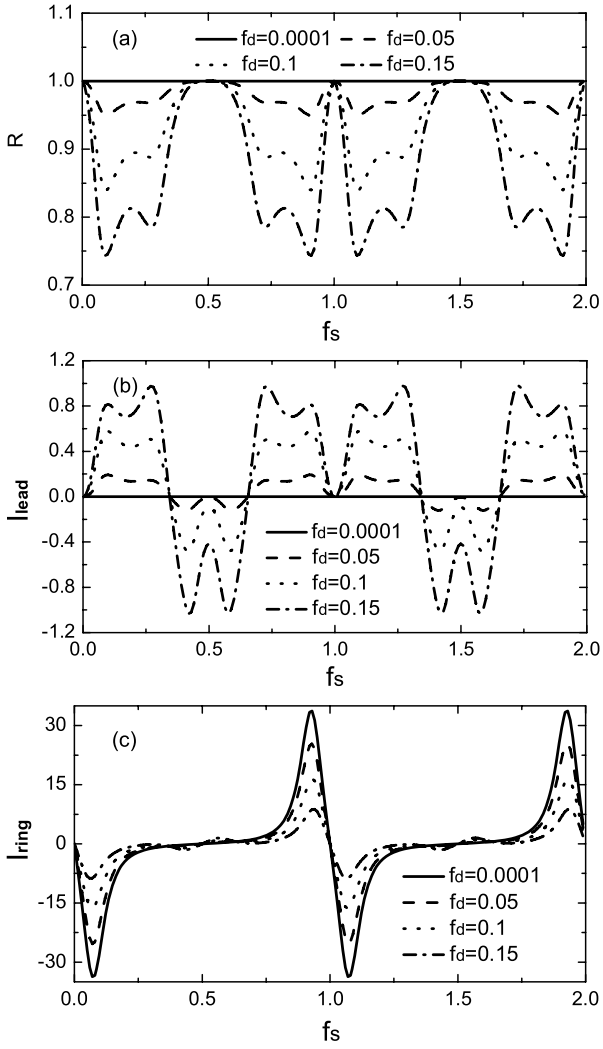

Figure 4. The reflection coefficient R (a), the average current I_{lead} in the lead (b), and the average current I_{ring} along the ring (c) (in units of $I_0 = e\hbar/(m_{\text{e}}L)$) versus the static magnetic flux f_{s}. Here the relevant parameters are taken as: $E = 2.2E_0$, $\hbar\omega = 2E_0$, $E_{\text{F}} = 5\hbar\omega$. It is clearly shown that when the amplitude of the dynamic flux is relatively small, $f_{\text{d}} = 0.0001$, $R \equiv 1$ and $I_{\text{ring}} \equiv 0$, which is the same as the phenomena of the ring driven by the static magnetic flux. However, increasing f_{d} makes the reflection coefficients and the average currents in the lead have much more obvious resonance owing to the stronger PAT process.

increases in the driving frequencies make the peaks of the average current (versus the static flux f_{s}) along the ring more obvious.

5. Conclusion and discussions

In conclusion, we used the quantum waveguide theory combined with the Floquet scattering theorem to investigate electron transport along an open mesoscopic ring (with one lead) driven by a time-periodic magnetic flux. We showed particularly that a current density wave could be excited along the open ring threaded by the time-periodic magnetic flux, and a net current could also be generated in the lead connected to only an electron reservoir. Basically, our numerical results showed that the amplitude of the dynamic fluxes can modulate

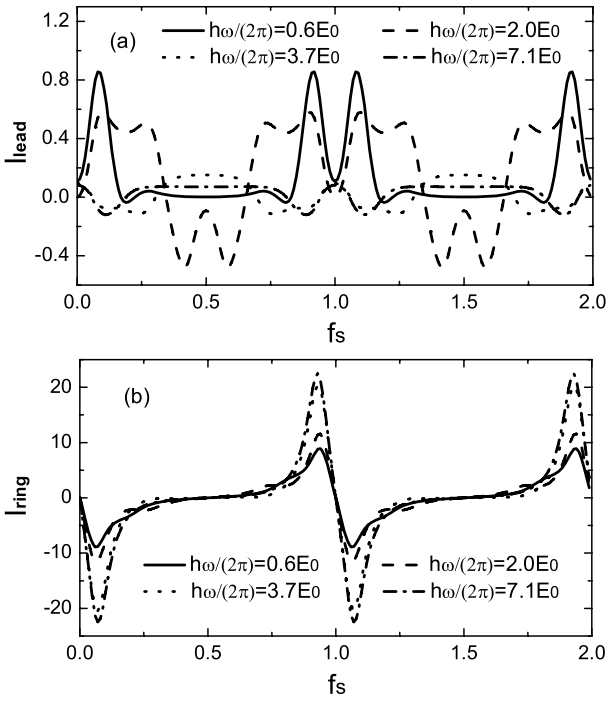

Figure 5. Time average current of the lead (a) and the ring (b) affected by photon-assisted tunnelings for different driven frequencies: $\omega = 0.6E_0/\hbar$, $2.0E_0/\hbar$, $3.7E_0/\hbar$, $7.1E_0/\hbar$, with $E = 2.2E_0$, $f_d = 0.1$, and $E_F = 5\hbar\omega$. It shows that the strong driven magnetic flux suppresses the PAT process.

the photon-assisted process between the lead and the ring. When the dynamic amplitude is relatively small, the electrons with different energies are reflected back to the lead and the current in the ring is not influenced. However, with the increase of the amplitude of the dynamic flux, the reflection coefficient could be less than unit. This is due to the interactions between the transported electrons and the applied oscillating external fields, by means of photon emissions and absorptions.

Note that superconducting quantum interference devices (SQUIDs) [35] and ultrasmall mechanical cantilevers [36] have already been successfully used to measure the weak currents (e.g. a few nano-amperes) in the mesoscopic structures. For the structure treated in the present work, one can choose $E_0 = \hbar^2\pi^2/(m_e L^2)$ as the unit of an electron's incident energy, so the unit of frequency is $\nu_0 = E_0/h$. Therefore, for the experimental ring of radius $R = 0.5$ μm, one can estimate $E_0 = 7.62 \times 10^{-8}$ eV, $\nu_0 = 18.42$ MHz. In fact, with the help of microwave resonators or wave guides [31], a time-period flux with such a frequency can be easily applied to the ring. Therefore, the current flowing along the lead can be controlled experimentally. In addition, a potential application of the model discussed in this paper is to design a switch to control the current in the lead by modulating the dynamic flux applied to the ring.

Acknowledgments

This work is partly supported by the NSFC (grant no. 10874142) and the Scientific Research Fund of SiChuan Provincial Education Department (grant no. 08zb021).

References

[1] Platero G and Aguado R 2004 *Phys. Rep.* **395** 1
[2] Tien P K and Gordon J P 1963 *Phys. Rev.* **129** 647
[3] Sollner T C L G, Goodhue W D, Tannenwald P E, Parker C D and Peck D D 1983 *Appl. Phys. Lett.* **43** 588
[4] Kouwenhoven L P, Jauhar S, Orenstein J, McEuen P L, Nagamune Y, Motohisa J and Sakaki H 1994 *Phys. Rev. Lett.* **73** 3443
[5] Drexler H, Scott J S, Allen S J, Campman K L and Gossard A C 1995 *Appl. Phys. Lett.* **67** 2816
[6] Keay B J, Allen S J Jr, Galán J, Kaminski J P, Campman K L, Gossard A C, Bhattacharya U and Rodwell M J W 1995 *Phys. Rev. Lett.* **75** 4098
Keay B J, Zeuner S, Allen S J Jr, Maranowski K D, Gossard A C, Bhattacharya U and Rodwell M J W 1995 *Phys. Rev. Lett.* **75** 4102
[7] Zhang C X, Nie Y H and Liang J Q 2006 *Phys. Rev.* B **73** 085307
[8] Ye C Z, Zhang C X, Nie Y H and Liang J Q 2007 *Phys. Rev.* B **76** 035345
[9] Sun Q F, Wang J and Lin T H 1999 *Phys. Rev.* B **59** 13126
[10] Zhao H K and Wang J 2006 *Phys. Rev.* B **74** 245401
[11] Orellana P A and Pacheco M 2007 *Phys. Rev.* B **75** 115427
[12] Shafranjuk S E 2007 *Phys. Rev.* B **76** 085317
[13] Trauzettel B, Blanter Y M and Morpurgo A F 2007 *Phys. Rev.* B **75** 035305
[14] Ahsan Zeb M, Sabeeh K and Tahir M 2008 *Phys. Rev.* B **78** 165420
[15] Shin D, Oymak H and Hong J 2007 *J. Phys.: Condens. Matter* **19** 226211
[16] Shin D and Hong J 2004 *Phys. Rev.* B **70** 073301
[17] Shin D and Hong J 2005 *Phys. Rev.* B **72** 113307
[18] Takai D and Ohta K 1993 *Phys. Rev.* B **48** 14318
[19] Benjamin C and Jayannavar A M 2001 *Phys. Rev.* B **64** 233406
[20] Arrachea L 2002 *Phys. Rev.* B **66** 045315
Arrachea L 2004 *Phys. Rev.* B **70** 155407
Foieri F, Arrachea L and Sánchez M J 2007 *Phys. Rev. Lett.* **99** 266601
[21] Büttiker M 1985 *Phys. Rev.* B **32** 1846
[22] Shirley J H 1965 *Phys. Rev.* **138** B979
[23] Holthaus M and Hone D 1993 *Phys. Rev.* B **47** 6499
[24] Fromherz T 1997 *Phys. Rev.* B **56** 4772
[25] Li W J and Reichl L E 1999 *Phys. Rev.* B **60** 15732
[26] Büttiker M and Landauer R 1982 *Phys. Rev. Lett.* **49** 1739
Büttiker M 1983 *Phys. Rev.* B **27** 6178
[27] Xia J B 1992 *Phys. Rev.* B **45** 3593
[28] Pareek T P and Jayannavar A M 1996 *Phys. Rev.* B **54** 6376
Joshi S K, Sahoo D and Jayannavar A M 2001 *Phys. Rev.* B **64** 075320
[29] Wei L F, Wang S J, Jia H Y and Jie Q L 1998 *Chin. Phys. Lett.* **15** 128
[30] Yi J, Wei J H, Hong J and Lee S I 2001 *Phys. Rev.* B **65** 033305
Park W and Hong J 2004 *Phys. Rev.* B **69** 035319
[31] Bulgakov E N and Sadreev A F 1995 *Phys. Rev.* B **52** 11938
[32] Bagwell P F and Lake R K 1992 *Phys. Rev.* B **46** 15329
[33] Abramowitz M and Stegun I A (ed) 1972 *Handbook of Mathematical Functions* (Washington, DC: National Bureau of Standards)
[34] Moskalets M and Büttiker M 2002 *Phys. Rev.* B **66** 245321
[35] Bluhm H, Koschnick N C, Bert J A, Huber M E and Moler K A 2009 *Phys. Rev. Lett.* **102** 136802
[36] Bleszynski-Jayich A C, Shanks W E, Peaudecerf B, Ginossar E, von Oppen F, Glazman L and Harris J G E 2009 *Science* **326** 272